Materials Research Proceedings 44 (2024) 569-579 https://doi.org/10.21741/9781644903254-61

Slider movement planning based on improved S-curve acceleration algorithms for servo presses

WANG Jun[1,a], WU Kai[1,b,*] and DING Wuxue[1,c]

[1]Nanjing University of Science and Technology, No. 200 Xiaolingwei Street, 210094 Nanjing, China

[a]wang-jun@njust.edu.cn, [b]wukai@njust.edu.cn, [c]wuxuexie@njust.edu.cn

Keywords: Slider Movement Planning, Servo Press, S-Curve, Deep Drawing Process

Abstract. Servo press is a forming equipment that uses a servo motor to drive a crank slider for stamping and deep drawing process. The servo drive can adjust the motor speed in real time and dynamically, which provides an important support for the dynamic adjustment of the crank slider movement. To realize the smooth reciprocating movement of the large-mass and high-inertia slider, it is necessary to develop a motor speed adjustment algorithm to achieve a good match between the movement load of the slider and the torque that the motor can bear, to ensure the operation safety of the whole machine. S-curve algorithms are often used for the planning of slider movement curves, which is easy to produce flexible impact on the motor. Therefore, to improve this situation, an improved S-curve algorithm is proposed based on the above common methods, which realizes the motion control method of smooth speed change. In this paper, a movement planning algorithm for servo press slider with improved S-curve is proposed based on the 7-phase S-curve acceleration algorithm. Firstly, the kinematic calculation of the crank slider mechanism is carried out. Secondly, 4 control points are set up to divide the slider movement curve of the typical drawing process, including the idle feed stage, deep drawing stage, idle return stage, and loading/unloading stage. Furthermore, the uniform acceleration stage and the uniform deceleration stage are removed, and the acceleration cusp was smoothed, and the improved S-curve algorithm was obtained. Finally, the large-scale crank slider servo press and its deep drawing parameters in a literature are taken as an example to solve the slider movement curves by using the improved S-curve. The results show that the improved S-curve algorithm can be used for servo press slide motion profile planning, which can realize efficient deep drawing process mode.

Introduction

With the rapid development of the manufacturing industry, the traditional mechanical press working mode is fixed, the motion characteristics cannot be adjusted, poor process adaptability and other defects, cannot meet the forming requirements of different materials and different stamping processes; on the other hand, with the development of servo control technology, servo motors are widely used. Compared with the traditional mechanical press, servo press has the advantages of flexibility, intelligence, high precision, low noise and high productivity [1-3]. By controlling the rotational speed of the servo motor, the motion characteristics of the slider can be effectively controlled, so that it can meet the requirements of different materials and different forming processes. The focus of the trajectory planning of the main drive mechanism of the servo press is the acceleration control of the main drive servo motor.

The current acceleration control algorithms mainly include S-curve acceleration [4-6], polynomial acceleration [7], trigonometric function acceleration [8], NURBS curve [9], Bezier curve [10,11], B-spline curve [12,13]. Among them, S-curve acceleration has abrupt changes in acceleration, and trigonometric and polynomial acceleration satisfy the requirements of acceleration and acceleration continuity, avoiding the flexural impact of machining [14]. Q. Hao [4] used S-curve to optimize the maximum acceleration of the trajectory. The maximum driving

force and the requirements of the motor were reduced. Z. Liu [5] used a 5-phase S-curve to optimize the amplitude of acceleration to suppress the torsional vibration of a synchronous belt-driven printing press system. X. Zhang [6] designed the traditional S-curve acceleration control model of the acceleration law change rule as a triangular shape, to solve the algorithm itself exists in the acceleration of the step of the problem. Q. Song [15] used the superposition of trigonometric functions of 2 different periods for acceleration model construction, thus reducing the requirement of motor power, but the algorithm fixed the time share of the variable speed interval.

In this paper starts from the common control algorithm of slider motion curve planning and proposes a servo press slider motion planning algorithm with improved S-curve. (1) Firstly, the kinematics calculation of crank slider mechanism is carried out to get the displacement, speed, acceleration over time curves and their relation equations; (2) Then, 4 control points are set to divide the typical deep drawing process curve into the idle feed stage, deep drawing stage, idle return stage, and loading/unloading stage, and the trend is illustrated; (3) Uniform acceleration stage and uniform deceleration stage in the S-curve algorithm are removed, and the acceleration cusps are smoothed, and an improved S-curve algorithm is obtained further to get the acceleration. The acceleration cusp is smoothed to obtain the improved S-curve algorithm, and the expressions of acceleration, speed and displacement over time are further obtained; (4) the parameters of crank-slider servo press in the reference paper are taken as an example, and the improved S-curve algorithm is used to plan and solve the slider motion curve.

Analysis of typical servo drawing process

Kinematic analysis of crank slider servo press. Taking the crank-slider press transmission system as an example, the kinematic analysis of the slider, its transmission mechanism and sketch are shown in Fig. 1(a) and 1(b), respectively, in which the eccentric crankshaft is the active part, and the connecting rod and the slider are the follower parts.

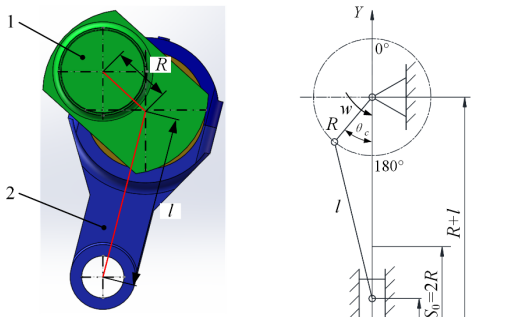

1. Eccentric crankshaft
2. Connecting rod
(a) Crank slider transmission mechanism

(b) Schematic diagram of the transmission mechanism

Fig. 1. Crank press drive system.

From Fig. 1(b), the relationship between the slider position, speed and acceleration and the crank angle can be established as follows:

$$S = R\left[(1-\cos\theta_c)+\frac{R}{4l}(1-\cos 2\theta_c)\right] \tag{1}$$

$$v = \frac{\mathrm{d}S}{\mathrm{d}t} = \omega R(\sin\theta_c + \frac{R}{2l}\sin 2\theta_c) \tag{2}$$

$$a = \frac{\mathrm{d}v}{\mathrm{d}t} = \frac{\mathrm{d}^2S}{\mathrm{d}t^2} = -\omega^2 R(\cos\theta_c + \frac{R}{l}\cos 2\theta_c) \tag{3}$$

Where, S is the stroke of the slider, mm; θ_c is the angle of the crank, °; R is the radius of the crank, mm; l is the length of the connecting rod, mm; v is the speed of the slider, mm/s; ω is the angular speed of the crank, rad/s; a is the acceleration of the slider, mm/s^2. When θ_c=0° (top dead centre, TDC)and θ_c=180° (bottom dead centre, BDC), there is a maximum acceleration a_{max}=-$w^2R(1+R/l)$. Further kinematic analysis using ADAMS yields the relationship between crank angle and slider displacement, speed and acceleration versus crank angle[16-17], as shown in Fig. 2.

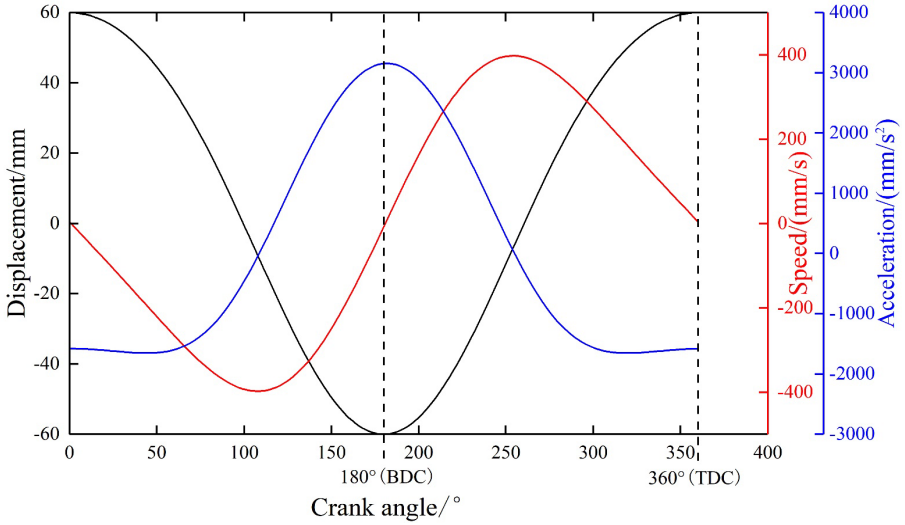

Fig. 2. Relation between slider displacement, speed, acceleration and crank angle.

Crank slider press, due to its structural parameters to determine, when the crank input constant speed, the slider movement parameters are also determined, when the slider is at the dead center, the acceleration will be a sudden change, easy to impact on the motor, affecting the stability of its normal function. Servo press can realize the dynamic adjustment of the output speed, to a certain extent, can avoid the slider in the dead position at the sudden change, so the crank slider servo press servo motor acceleration control, to realize the smooth transition of the slider speed, acceleration.

Analysis of servo drawing process curve. Taking a servo drawing process curve as an example, 4 control points are set up to divide the slider movement curve of the typical drawing process, including the idle feed stage I, deep drawing stage II, idle return stage III, and loading/unloading stage IV, as shown in Fig. 3. Where the slider runs to the idle feed stage I, the slider first accelerated and then decelerated, there is a maximum speed; when the slider runs to the deep drawing stage II, the slider is a uniform speed; when the slider runs to the idle return stage III, the slider has a sharp return characteristics, the speed is gradually reduced; when the slider runs to the loading/unloading stage IV, the slider runs to the top dead centre near the lower speed, for the loading and unloading to set aside a longer period of time for the manipulator to carry out loading and unloading operation.

Materials Research Proceedings 44 (2024) 569-579 https://doi.org/10.21741/9781644903254-61

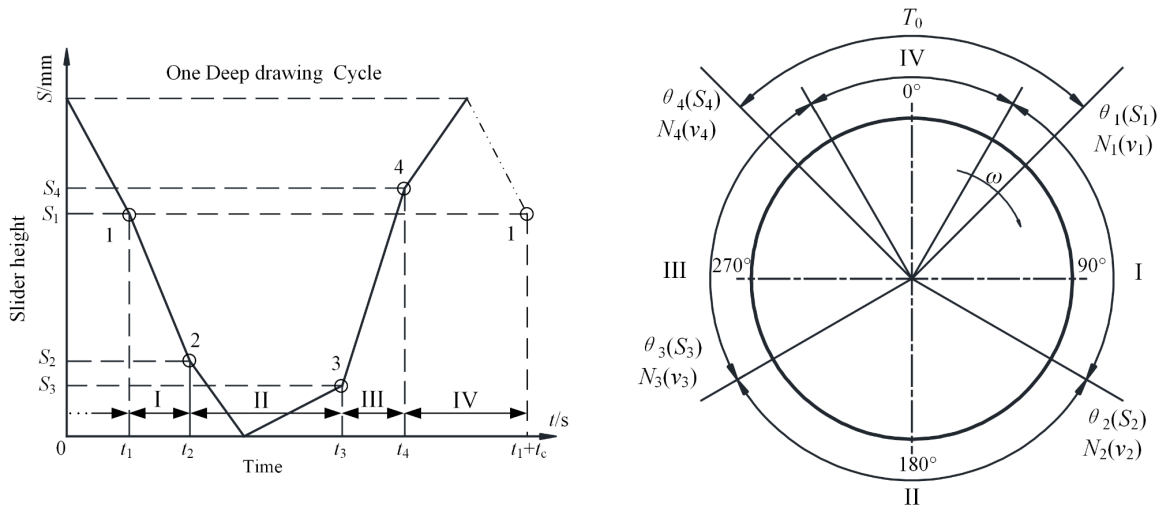

Fig.. 3. Typical deep drawing process for servo presses.

Key point 1: Slider closing angle θ_1, according to the transmission system can determine the slider position S_1, θ_1 is the corresponding crank angle when the robot transfers the blank to the forming and then safely leaves the press; S_1 is the corresponding slider safety height; N_1 is the corresponding crank instantaneous speed; v_1 is the corresponding slider instantaneous speed. Key point 2: the stamping start angle θ_2 and stamping start rotational speed N_2, according to the transmission system, the height of the slide S_2 and speed v_2 can be calculated, where θ_2 is the crank angle when the press starts stamping; N_2 is the corresponding crank rotational speed; S_2 is the initial height of the part when the press starts stamping; v_2 is the speed of the slide when the part starts

stamping. Key point 3: the stamping end angle θ_3 and stamping end rotational speed N_3, according to the transmission system can be calculated slider height S_3 and speed v_3, where θ_3 is the crank angle at the end of the die pulling; N_3 is the corresponding crank rotational speed at the end of the die pulling; S_3 is the height of the die pulling/slider contacting the height of the part; v_3 is the speed of slider at the end of the die pulling. Where N_2=N_3. Key point 4: the slider opening angle θ_4, according to the transmission system can be calculated slider height S_4 and speed v_4, where θ_4 is the corresponding crank angle when the manipulator leaves the press after picking up the workpiece; S_4 is the height of the corresponding slider; N_4 is the instantaneous rotational speed of the corresponding crank; and v_4 is the instantaneous speed of the corresponding slider.

The T_0 is the safety time required for the press manipulator to remove the workpiece and place the blank, the time required for the crank to run from θ_4 to θ_1, during which the manipulator is required to complete the removal of the workpiece, the transfer of the blank, and leave the press safely.

Principle of improved S-curve acceleration algorithm

Principle of 7- phase S-curve acceleration algorithm. S-curve acceleration algorithm is a commonly used algorithm for controlling the object under test to realize smooth acceleration, uniform speed and deceleration process, to ensure the smoothness and stability of the mechanical system when the motor starts, stops, and moves at a constant speed. S-curve acceleration consists of 7 segments, acceleration, uniform acceleration, deceleration, uniform speed, acceleration, uniform deceleration, and deceleration segments, shown in Fig. 4.

Materials Research Proceedings 44 (2024) 569-579 https://doi.org/10.21741/9781644903254-61

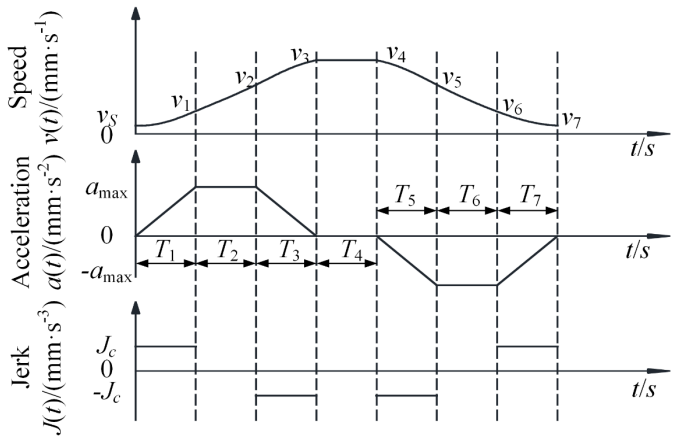

Fig. 4. S-curve acceleration principle.

Define the following variables:

$$T_k = t_k - t_{k-1}\left(k = 1,2,3,4,5,6\right) \tag{4}$$

$$\tau_k = t - t_{k-1}\ \left(k = 1,2,3,4,5,6\right) \tag{5}$$

$$T_1 = T_3 = T_5 = T_7; T_2 = T_4 = T_6 \tag{6}$$

$$JT_1 = a_{max} \tag{7}$$

Combining Fig. 4 and Eq. 4 to Eq. 7, the equations for acceleration, speed and time in the S-curve acceleration algorithm can be clarified as Eq. 8 to Eq. 9.

$$a(t) = \begin{cases} J_C\tau_1, & 0 < t \le t_1 \\ J_C T_1, & t_1 < t \le t_2 \\ J_C T_1 - J_C\tau_3, & t_2 < t \le t_3 \\ 0, & t_3 < t \le t_4 \\ -J_C\tau_5, & t_4 < t \le t_5 \\ -J_C T_1, & t_5 < t \le t_6 \\ -J_C T_1 + J_C\tau_7, & t_6 < t \le t_7 \end{cases} \tag{8}$$

$$v(t) = \begin{cases} v_S + \frac{1}{2}J_C\tau_1^2, & 0 < t \le t_1,\ t = t_1,\ v_1 = v_S + \frac{1}{2}J_C T_1^2 \\ v_S + \frac{1}{2}J_C T_1^2 + J_C T_1\tau_2, & t_1 < t \le t_2,\ t = t_2,\ v_2 = v_S + \frac{1}{2}J_C T_1^2 + J_C T_1 T_2 \\ v_S + \frac{1}{2}J_C T_1^2 + J_C T_1 T_2 + J_C T_1\tau_3 - \frac{1}{2}J_C\tau_3^2, & t_2 < t \le t_3,\ t = t_3,\ v_3 = v_S + J_C T_1 T_2 + J_C T_1^2 \\ v_S + J_C T_1^2 + J_C T_1 T_2 & t_3 < t \le t_4,\ t = t_4,\ v_4 = v_S + J_C T_1 T_2 + J_C T_1^2 \\ v_S + J_C T_1^2 + J_C T_1 T_2 - \frac{1}{2}J_C\tau_5^2, & t_4 < t \le t_5,\ t = t_5,\ v_5 = v_S + \frac{1}{2}J_C T_1^2 + J_C T_1 T_2 \\ v_S + \frac{1}{2}J_C T_1^2 + J_C T_1 T_2 - J_C T_1\tau_6, & t_5 < t \le t_6,\ t = t_6,\ v_6 = v_S + \frac{1}{2}J_C T_1^2 \\ v_S + \frac{1}{2}J_C T_1^2 - J_C T_1\tau_7 + \frac{1}{2}J_C\tau_7^2, & t_6 < t \le t_7,\ t = t_7,\ v_7 = v_S \end{cases} \tag{9}$$

By setting the time of acceleration, deceleration, acceleration and deceleration segments in the 7-phase S-curve acceleration algorithm equal to the time of acceleration, deceleration, acceleration and deceleration segments, and the time of uniform acceleration, uniform speed and uniform

deceleration segments, the solution of speed can be simplified, and it can also ensure that the initial speed v_0 is equal to the final speed v_7 after the acceleration algorithm is run as shown in Eq. 9.
Principle of improved S-curve acceleration algorithm. Due to the specific machining process, the slider by the acceleration algorithm run by the beginning and end of the speed is not equal, and it may introduce many different time divisions of the S-curve acceleration algorithm, which will have many parameters. Therefore, the 7-phase S-curve acceleration algorithm is improved, the uniform acceleration section and acceleration/deceleration section are removed, while the uniform speed section in the middle section is moved to the two ends of the acceleration section, deceleration section next to the curve, and at the same time the curve obtained is smoothed by using a quadratic parabola at the acceleration mutation cusp, and the schematic diagram is shown in Fig. 5.

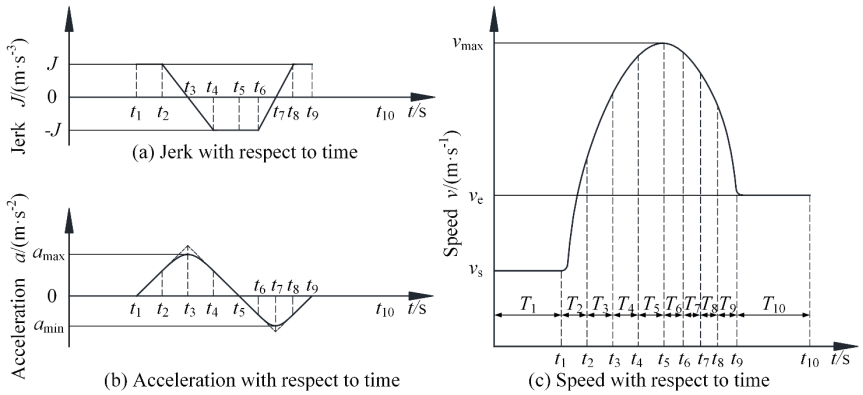

Fig. 5. Improved S-curve acceleration algorithm principle schematic diagram.

To simplify the solution, the following conditions are assumed here: $T_2=T_3=T_4=T_5$, $T_6=T_7=T_8=T_9$, then $v_S \neq v_e$; If $T_2=T_3=T_4=T_5=T_6=T_7=T_8=T_9$, then $v_S=v_e$. Therefore, taking $v_S \neq v_e$ as an example, the relations between acceleration, acceleration, speed and time of the improved S-curve acceleration algorithm are given, as shown in Eq.10 to Eq.12.

$$J(t)=\begin{cases} 0, & 0<t\le t_1 \\ J, & t_1<t\le t_2 \\ J-\dfrac{J}{T_3}\tau_3, & t_2<t\le t_3 \\ -\dfrac{J}{T_4}\tau_4, & t_3<t\le t_4 \\ -J, & t_4<t\le t_5 \\ -J, & t_5<t\le t_6 \\ \dfrac{J}{T_7}\tau_7-J, & t_6<t\le t_7 \\ \dfrac{J}{T_8}\tau_8, & t_7<t\le t_8 \\ J, & t_8<t\le t_9 \\ 0, & t_9<t\le t_{10} \end{cases} \tag{10}$$

Further integration yields an expression for the acceleration -time relationship as follows.

$$a(t)=\begin{cases}0, & 0<t\le t_1\\ J\tau_2, & t_1<t\le t_2, t=t_2, a_2=JT_2\\ J(T_2+\tau_3-\frac{\tau_3^2}{2T_3}), & t_2<t\le t_3, t=t_3, a_3=\frac{3}{2}JT_2\\ J(\frac{3}{2}T_2-\frac{\tau_4^2}{2T_2}), & t_3<t\le t_4, t=t_4, a_4=JT_2\\ J(T_2-\tau_5), & t_4<t\le t_5, t=t_5, a_5=0\\ -J\tau_6, & t_5<t\le t_6, t=t_6, a_6=-JT_6\\ J(-T_6+\frac{\tau_7^2}{2T_6}-\tau_7), & t_6<t\le t_7, t=t_7, a_7=-\frac{3}{2}JT_6\\ J(-\frac{3}{2}T_6+\frac{\tau_8^2}{2T_6}), & t_7<t\le t_8, t=t_8, a_8=-JT_6\\ J(-T_6+\tau_9), & t_8<t\le t_9, t=t_9, a_9=0\\ 0, & t_9<t\le t_{10}, t=t_{10}, a_{10}=0\end{cases} \tag{11}$$

Further integration yields an expression for the speed-time relationship as follows.

$$v(t)=\begin{cases}v_s, & 0<t\le t_1, t=t_1, v_1=v_s\\ v_s+\frac{1}{2}J\tau_2^2, & t_1<t\le t_2, t=t_2, v_2=v_s+\frac{1}{2}JT_2^2\\ v_s+\frac{1}{2}JT_2^2+J(T_2\tau_3+\frac{1}{2}\tau_3^2-\frac{\tau_3^3}{6T_3}), & t_2<t\le t_3, t=t_3, v_3=v_s+\frac{11}{6}JT_2^2\\ v_s+\frac{11}{6}JT_2^2+J(\frac{3}{2}T_2\tau_4-\frac{\tau_4^3}{6T_2}), & t_3<t\le t_4, t=t_4, v_4=v_s+\frac{19}{6}JT_2^2\\ v_s+\frac{19}{6}JT_2^2+J(T_2\tau_5-\frac{1}{2}\tau_5^2), & t_4<t\le t_5, t=t_5, v_5=v_s+\frac{11}{3}JT_2^2\\ v_s+\frac{11}{3}JT_2^2-\frac{1}{2}J\tau_6^2, & t_5<t\le t_6, t=t_6, v_6=v_s+\frac{11}{3}JT_2^2-\frac{1}{2}JT_6^2\\ v_s+\frac{11}{3}JT_2^2-\frac{1}{2}JT_6^2-J(T_6\tau_7-\frac{\tau_7^3}{6T_6}+\frac{1}{2}\tau_7^2), & t_6<t\le t_7, t=t_7, v_7=v_s+\frac{11}{3}JT_2^2-\frac{11}{6}JT_6^2\\ v_s+\frac{11}{3}JT_2^2-\frac{11}{6}JT_6^2-J(\frac{3}{2}T_6\tau_8-\frac{\tau_8^3}{6T_6}), & t_7<t\le t_8, t=t_8, v_8=v_s+\frac{11}{3}JT_2^2-\frac{19}{6}JT_6^2\\ v_s+\frac{11}{3}JT_2^2-\frac{19}{6}JT_6^2-J(T_6\tau_9-\frac{1}{2}\tau_9^2), & t_8<t\le t_9, t=t_9, v_9=v_s+\frac{11}{3}JT_2^2-\frac{11}{3}JT_6^2\\ v_s+\frac{11}{3}JT_2^2-\frac{11}{3}JT_6^2, & t_9<t\le t_{10}, t=t_{10}, v_e=v_s+\frac{11}{3}JT_2^2-\frac{11}{3}JT_6^2\end{cases} \tag{12}$$

The above parameters $a_{\max}$、$a_{\min}$、T_f、$v_{\max}$、v_s、v_e are the key parameters in the process curve, which can be used to express the control parameters in the process of S-curve acceleration algorithm, such as: time interval T_i, the jerk J and other parameters, which can simplify the acceleration algorithm in the solution, according to the boundary conditions can be obtained in part of the parameters of the relationship between the Eq.13 to Eq. 21.

$$v_{\max}=v_5=v_s+\frac{11}{3}JT_2^2 \tag{13}$$

$$J=\frac{2a_{\max}}{3T_2}=-\frac{2a_{\min}}{3T_6}=\frac{44a_{\max}^2}{27(v_{\max}-v_s)}=-\frac{44a_{\min}^2}{27(v_{\max}-v_e)} \tag{14}$$

$$T_2=T_3=T_4=T_5=\frac{9(v_{\max}-v_s)}{22a_{\max}} \tag{15}$$

$$T_6 = T_7 = T_8 = T_9 = -\frac{9(v_{\max} - v_e)}{22a_{\min}} \tag{16}$$

$$a_{\min} = a_7 = -\frac{3}{2}JT_6 = -\frac{T_6}{T_2}a_{\max} \tag{17}$$

$$T_1 = T_{10} = \frac{T_f}{2} - \frac{2(a_{\max} - a_{\min})T_2}{a_{\max}} = \frac{T_f}{2} - \frac{9a_{\min}(v_{\max} - v_s) - 9a_{\max}(v_{\max} - v_e)}{11a_{\max}a_{\min}} \tag{18}$$

$$v_e = v_s + \frac{11}{3}JT_2^2 - \frac{11}{3}JT_6^2 \tag{19}$$

$$T_f = \sum_{i=1}^{10} T_i, \quad i = 1,2,3,...,10 \tag{20}$$

$$a_{\max} = a_3 = \frac{3}{2}JT_2 \tag{21}$$

Trajectory planning of servo motor press

Trajectory planning model establishment. According to the previous analysis of the servo press drive system and the deep-drawing process curve, the angular speed, angular acceleration and angular jerk curve of the servo motor in the complete cycle of the deep-drawing process are given, as shown in Fig. 6. The relevant variables in the improved S-curve acceleration control algorithm can be determined according to the process parameters in the actual case. The selected range of angular speed extreme angles, x_1, x_2, x_3, and x_4, is determined based on θ_1, θ_2, θ_3, and θ_4. Where θ_1, θ_2, θ_3, and θ_4, and w_1, w_2, and w_3 are known variables, angular speed extremes angles x_1, x_2, x_3, and x_4, angular speed extremes w_{m1}, and w_{m2}, angular acceleration extremes angles y_1, y_2, y_3, and y_4 and known angles θ_1, θ_2, θ_3, and θ_4 in the interval time/angle T_0, T_1, T_2, T_3, T_4, T_5, T_6, T_7, T_8, T_9, T_{10}, T_{11}, T_{12}, T_{13}, T_{14}, T_{15}, T_{16}, and T_{17} are unknown parameters and need to be solved. The following relationship exists for the interval time/angle: $T_1=T_2=T_3=T_4$; $T_5=T_6=T_7=T_8$; $T_{10}=T_{11}=T_{12}=T_{13}$; $T_{14}=T_{15}=T_{16}=T_{17}$. There is also $w_2=w_3$.

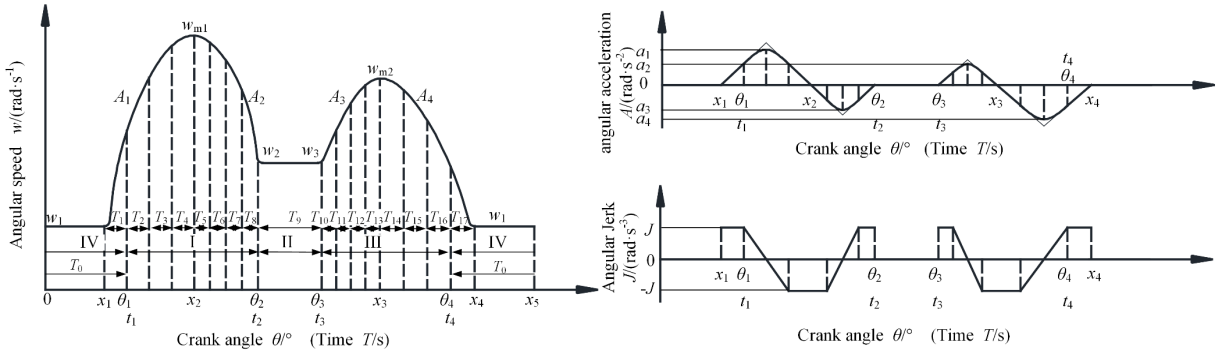

Fig. 6. Angular speed curve and key points of servo motor throughout the whole week.

From the Fig. 6, in the idle feed stage, the crank is first accelerated by acceleration A_1 from w_1 to the angular speed extremes w_{m1}, and then decelerated by acceleration A_2 from w_{m1} to the starting speed of the stamping w_2; into the deep drawing stage, the crank is deep-drawn at a constant speed of w_2 until the end of the θ_3; and then into the idle return stage, the crank is first accelerated by acceleration A_3 from w_3 to the angular speed extremes w_{m2}, and then decelerated by acceleration

A_4 from w_{m2} to w_1 in order to achieve the upper dead center of the low-speed operation, and so on to realize the continuous stamping operation.

Slider motion trajectory planning solution. Taking the relevant parameters of a certain type of servo press in the references as an example, solving the speed trajectory planning and compare the results with those in the references [18]. The relevant parameters of the servo press are as follows: crank radius R=450 mm, connecting rod length L=1200 mm, and slider stroke S=900 mm, and the process control parameters are set up as an example for the deep drawing forming of a certain model's side panel, in which the forming height of the part is 200 mm, and the speed of the start of the deep drawing process is required to be less than 300 mm/s, and the height of the safety space required by the manipulator is not less than 700 mm, and the transfer time is not less than 2 s, the speed of die pulling is less than 80 mm/s when the height of die pulling is 10 mm, and the maximum acceleration of slider is less than 3500 mm/s^2. The key point control parameters are set as follows: θ_1=66°, θ_4=294°, S_1=S$_4$=705.7 mm, T_0=2s; θ_2=131.5°, S_2=200.1 mm, w_2=w_3=6.7 rpm, v_2=297.7 mm/s, θ_3=190°, S_3=9.4 mm, v_3=75.1 mm/s.

As shown in Fig. 6, the following relationships exist for some parameters: $x_1+T_1=t_1/\theta_1$; $t_1/\theta_1+T_1=y_1$; $x_1+4T_1=x_2$; $x_2+2T_5=y_2$; $x_2+4T_5=t_2/\theta_2$; $t_2/\theta_2+T_9=t_3$; $t_3/\theta_3+2T_{10}=y_3$; $t_3/\theta_3+4T_{10}=x_3$; $x_3+2T_{14}=y_4$; $x_3+3T_{14}=t_4/\theta_4$; $t_4/\theta_4+T_{14}=x_4$. Where the solution parameters include X=[x_1, x_2, x_3, x_4, x_5, w_{m1}, w_{m2}, T_1, T_5, T_9, T_{10}, T_{14}, J], and hence a set of solutions X_0=[0.9, 1.3, 3.24, 4.14, 5.14, 22.5, 24.5, 0.1, 0.11, 1.4, 0.125, 0.1, 313.63], and the corresponding crank and slider kinematic parameter plots can be obtained, as shown in Figs. 7, 8, and 9.

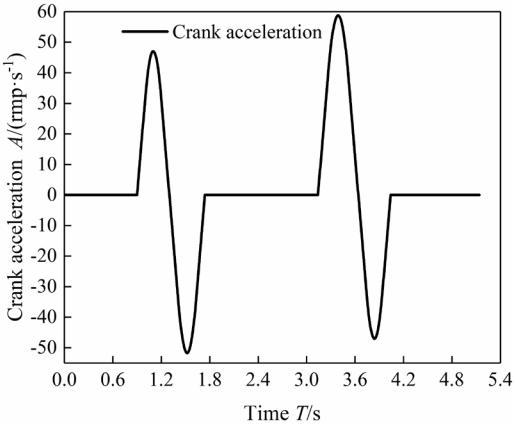

Fig. 7. Slider height and crank speed curve.

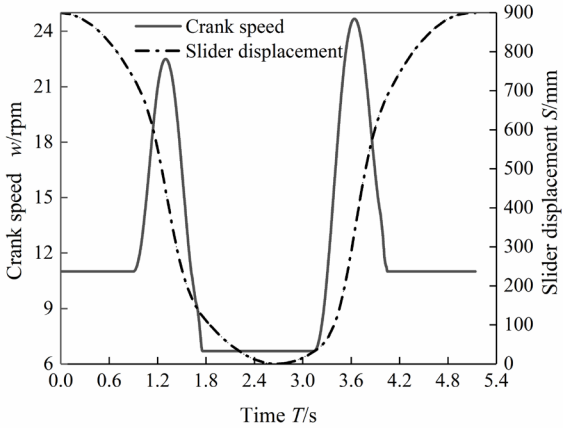

Fig. 8. Crank acceleration curve.

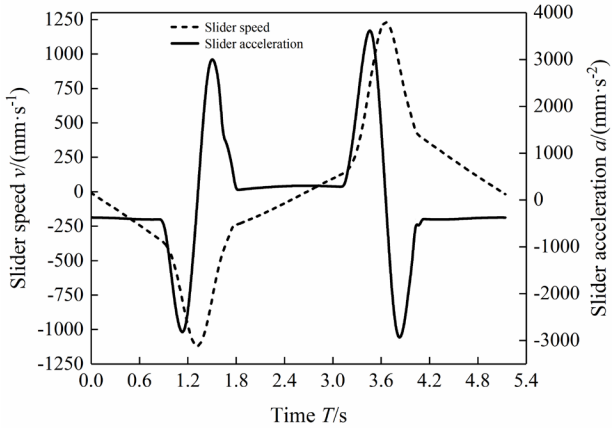

Fig. 9. Slider speed and acceleration curve.

Fig. 7, 8, and 9 illustrate that while satisfying the spatial and temporal constraints of the transfer manipulator and the maximum acceleration of the press slider, the maximum production rate can reach 11.7 times/min. This significantly enhances production efficiency. The continuous variation

of crank acceleration depicted in Fig. 8 and 9 ensures reliable equipment operation with heightened flexibility. These findings underscore the efficacy of the improved S-curve acceleration algorithm for planning the motion curve of the servo press slider.

Summarize

An efficient deep drawing process mode of servo press is established, and the servo press machining process trajectory planning can be realized by setting 4 key point control parameters, which is simple and convenient to set up and easy to operate on site. The servo motor flexible acceleration and deceleration control algorithm with improved S- curve is proposed, and the crank speed, acceleration and acceleration changes are continuous, which avoids the impact of acceleration and deceleration process on the equipment, and it can be used for servo press deep drawing trajectory planning.

References

[1] F. Peng, C. Wang, H. Chai, Z. Shao, S. Wang, B. Wang, Lightweight slider design for a servo press based on its layered structure, J. Tsinghua Univ. (Sci. Technol.) 12 (2020) 1016-1022. https://doi.org/10.16511/j.cnki.qhdxxb.2020.22.016

[2] F. Peng, P. Zhang, L. Wang, Z. Shao, D. Yang, K. Yang, Energy management of servo press lines based on flywheel speed adaptive planning, J. Tsinghua Univ. (Sci. Technol.) 11 (2020) 927-933. https://doi.org/10.16511/j.cnki.qhdxxb.2020.22.014

[3] L. Yang, S. Xu, W. Shi, H. GE, Research on S Type Acceleration and Deceleration Time Planning Algorithm with Beginning and End Speed Non-zero, J. Mech. Eng. 23 (2016) 199-206. https://doi.org/10.3901/JME.2016.23.199

[4] Q. Hao, L. Guan, L. Wang, Intelligent acceleration/deceleration control algorithm for drive force for a heavy duty hybrid machine tool, J. Tsinghua Univ. (Sci. Technol.). 11 (2020) 1770-1773, 1778. https://doi.org/10.3321/j.issn:1000-0054.2009.11.009

[5] Z. Liu, S. Zhang, L. Cai, J. Yang, B. Xu, P. Xu, Five-phase S-curve Control Method Based on Particle Swarm Optimization, J. Beijing Univ Technol. 5 (2015) 641-648. https://doi.org/10.11936/bjutxb2014060067

[6] X. Zhang, D. Zhu, F. Pan, Research on S-curve flexible Acc/Dec control algorithm in NC machining, Manuf. Autom. 12 (2020) 68-73. https://doi.org/10.3969/j.issn.1009-0134.2020.12.014

[7] J. Chen, S.S. Yeh, J. Sun, An S-curve Acceleration/Deceleration Design for CNC Machine Tools Using Quintic Feedrate Function, Comput - Aided Des & Appl. 4 (2011) 583-892. https://doi.org/10.3722/cadaps.2011.583-592

[8] X. Guo, C. Li, A New Flexible Acceleration and Deceleration Algorithm, Journal of Shanghai Jiaotong University. 2 (2003) 205-207. https://doi.org/10.3321/j.issn:1006-2467.2003.02.016

[9] Y. Chen, W. Guo, F. Gao, NURBS-Based Feature Modeling and Trajectory Planning for Ram Motion of Servo Mechanical Presses, J. Shanghai Jiaotong Univ. 1 (2009) 138-142. https://doi.org/10.3321/j.issn:1006-2467.2009.01.031

[10] X. Qu, Design and simulations of non-uniform speed motion curves for a slider-crank servo press, Assem. Autom. 3 (2018) 336-346. https://doi.org/10.1108/AA-10-2016-131

[11] W. Shang, S. Zhao, Servo Press Processing Bezier-Model with Optimum, J. Xi'an Jiaotong Univ. 3 (2012) 31-35.

[12] J. Gu, T. Wu, C. Li, B. Zhang. Y. Zhang, Trajectory Fairing Algorithm for Shrub Pruning Based on Improved Cubic B-spline, Trans. Chin. Soc. Agric. Mach. S1 (2021) 89-97. https://doi.org/10.6041/j.issn.1000-1298.2021.S0.012.

[13] P. Cheng, P. Chen, Y. Lin, Small mechanical press with double-axis servo system for forming of small metal products, Int. J. Adv. Manuf. Technol. 68 (2013) 2371-2381. https://doi.org/10.1007/s00170-013-4851-y

[14] H. Luo, The Research on Interpolation Algorithm of NURBS Curve Based on Milne-Hamming Method and Acceleration/Deceleration Control Algorithm, Nanjing: Nanjing University of Aeronautics and Astronautics, 2020.

[15] Q. Song, B. Guo, J. Li, W. Yin, Flexible Acceleration and Deceleration Control Algorithm for Servo Press, Trans. Chin. Soc. Agric. Mach. 6 (2013) 269-273. https://doi.org/10.6041/j.issn.1000-1298.2013.06.047

[16] H Lin, D Ye, X Wang, Y Liu, Motion planning of main drive system of high speed fine blanking press by double servo drive, J. Huazhong Univ. Sci. Technol. 4 (2018) 6-11. https://doi.org/10.13245/j.hust.180402

[17] Y. Sun, J. Hu. Y. Cheng, W. Ruan, Characteristics Analysis of Working Mechanisms for Servo Mechanical Presses, Appl. Mech. Mater. 220-223 (2012) 762-767. https://doi.org/10.4028/www.scientific.net/AMM.220-223.762

[18] W. Yin, J. Li, Q. Song, Planed and Optimized Drawing Trajectory for Heavy Servo Presses, CFHI Technol. 1 (2015) 1-5. https://doi.org/10.3969/j.issn.1673-3355.2015.01.001